

# VISCOELASTICITY OF BIOPOLYMER NETWORKS AND STATISTICAL MECHANICS OF SEMIFLEXIBLE POLYMERS

ERWIN FREY, KLAUS KROY AND JAN WILHELM

---

<b>I</b>	<b>INTRODUCTION</b>	<b>2</b>
<b>II</b>	<b>STATICS AND DYNAMICS OF SINGLE FILAMENTS</b>	<b>4</b>
II.A	Linear force-extension relation . . . . .	5
II.B	Nonlinear response . . . . .	6
II.C	Single filament dynamics . . . . .	9
II.C.1	Dynamic light scattering . . . . .	11
II.C.2	Colloidal probes and micro-rheology . . . . .	14
<b>III</b>	<b>VISCOELASTICITY OF BIOPOLYMER NETWORKS</b>	<b>15</b>
III.A	Experimental techniques and results . . . . .	15
III.A.1	Macro-rheology . . . . .	15
III.A.2	Micro-rheology . . . . .	17
III.B	Theoretical modeling . . . . .	18
III.B.1	Typical length and time scales; the tube picture . . . . .	20
III.B.2	The “rubber plateau” . . . . .	22
III.B.3	Terminal relaxation . . . . .	27
III.B.4	High frequency behavior . . . . .	28
III.B.5	Effect of crosslinking . . . . .	31
<b>IV</b>	<b>CONCLUSIONS AND OPEN PROBLEMS</b>	<b>33</b>

*Review published in Advances in Structural Biology (Vol.5), edited by S.K. Mathotra and J.A. Tuszynski, (Jai Press, London, 1998).*

## I INTRODUCTION

A central problem in molecular cell biology is the understanding of the factors that determine and regulate the structure and mechanical properties of cells (Hesketh and Pryme, 1995). For instance monolayers of endothelial cells when stimulated with laminar shear stress exhibit changes in morphology that activate gene expression (Dewey et al., 1981; Satcher and Dewey, 1996). There is a plenitude of other cellular phenomena, where the material properties of cells play a vivid role. These range from cell motility to cell growth and division and active intracellular transport.

The structure responsible for the mechanical properties of the cell is the *cytoskeleton*, a rigid yet flexible and dynamic network of proteins of varying length and stiffness. Most cells contain three types of protein filaments comprised of actin, tubulin and intermediate filament proteins such as vimentin. These, as well as the plasma-membrane associated filaments make up the *cytoskeleton* (Schliwa, 1985). Together with a large variety of additional proteins which act as cappers, cross-linkers and bundlers it constitutes a composite system with a wide variety of material properties which may easily be changed. On the one hand there is the extremely well organized and stably structured actin cytoskeleton in a striated muscle cell. On the other hand we have the very dynamic cytoskeleton in motile cells like leukocytes, fibroblasts and other cell types that migrate individually on a surface or through tissues. It is absolutely essential for these cells to be able to reorganize the cytoskeleton efficiently and fast, otherwise it would not be possible to fight against bacterial and viral infections, to undergo chemotaxis during muscle regeneration, or even to perform normal cytokinesis. Hence it is of considerable relevance in cell biology to understand the factors that determine and regulate the viscoelasticity of the cytoskeletal network.

Actin filaments seem to be of particular importance for the viscoelastic properties of the cytoplasm. They are distributed throughout the cell and give the appearance of a gel network when observed by electron microscopy (see Fig. 1). F-actin which is a double-stranded helical filament made up of G-actin monomers has several quite remarkable properties: (1) It is a self-assembling protein which in buffers of physiologic ionic strength spontaneously starts to assemble from the globular actin subunits. (2) There is a great variety of actin associated proteins ( $\alpha$ -actinin, myosin, gelsolin etc.) which regulate the average filament length and the assembly (e.g. the degree of crosslinking) of F-actin in the cytoskeleton. (3) F-actin has a remark-

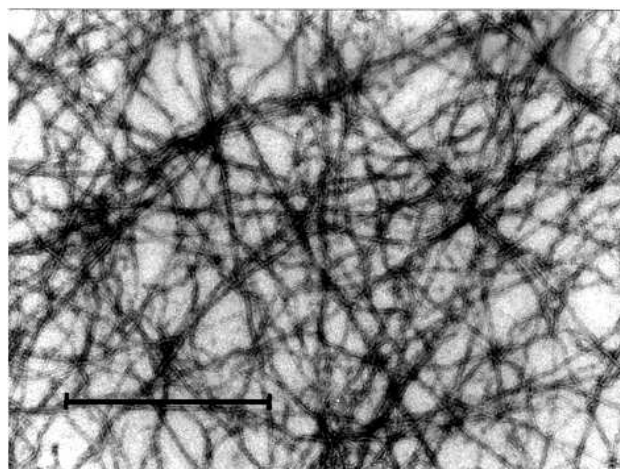


Figure 1: Electron micrograph of a 0.4 mg/ml actin solution polymerized in vitro. The bar indicates the length of 1  $\mu\text{m}$ .

ably stiff structure with a persistence length comparable to the total contour length.

From a physicist point of view the main motivation for investigating the viscoelastic properties of F-actin networks stems from the fact that they provide versatile model systems to study fundamental properties of polymeric fluids and gels. One major difference to synthetic polymers is the enormous length of these filaments – *in vitro* actin can form filaments up to 50  $\mu\text{m}$  in length – and their large persistence length of  $\ell_p \approx 17\mu\text{m}$ . Thus actin filaments are a very good realization of *semiflexible polymers* whose material and statistical properties are very different from Gaussian chains. First of all their response to an external force is not isotropic but depends on the direction with respect to the mean contour. Second, the statistical mechanics (e.g. the distribution function for the end-to-end vector) of such macromolecules cannot be understood from conformational entropy alone but crucially depends on the bending stiffness of the filaments. Unlike flexible polymers, for which we have quite a complete theoretical picture (Yamakawa, 1971; des Cloizeaux and Jannink, 1990; Doi and Edwards, 1986), the statistical mechanics of semiflexible extended objects is still a field with many challenging theoretical problems. Recent advances in this area will be discussed in section II.

The mechanical properties of single filaments can be expected to be con-

stitutive for the *collective* mechanical properties of gels and sufficiently concentrated solutions of semiflexible polymers. These are interesting polymeric systems with rheological properties that can not be accounted for by the classical theory of rubber elasticity (Treloar, 1975; Ferry, 1980). They exhibit an elastic plateau already at remarkably low volume fractions, show strain hardening and other anomalous material properties which will be discussed in detail in section III. Studying the viscoelastic properties of F-actin networks *in vitro* is certainly a prerequisite for a deeper understanding of the mechanical properties of biological tissue.

## II STATICS AND DYNAMICS OF SINGLE FILAMENTS

Recent advances in visualizing and manipulating single polymer chains directly have provided unique experimental tools for studying the static and dynamic properties of individual strands of F-actin (Nagashima and Asakura, 1980; Kishino and Yanagida, 1992; Gittes et al., 1993; Käs et al., 1993; Ott et al., 1993; Käs et al., 1996). Further insight into the structural and dynamic properties can also be gained from micro-rheology (Ziemann et al., 1994) and dynamic light-scattering (Schmidt et al., 1989; Götter et al., 1996) of macromolecular networks. Due to this variety of experimental methods it became possible to check the validity of theoretical models for the statics and dynamics of single semiflexible polymers.

The model usually adopted for a theoretical description of semiflexible chains like actin filaments is the *wormlike chain model* (Kratky and Porod, 1949; Saitô et al., 1967). Here the filament is represented by an inextensible space curve  $\mathbf{r}(s)$  of total length  $L$  parameterized in terms of the arc length  $s$ . The statistical properties of the wormlike chain are determined by a free energy functional  $H$  which measures the total elastic energy of a particular conformation

$$H = \int_0^L ds \frac{\kappa}{2} \left( \frac{\partial \mathbf{t}}{\partial s} \right)^2 ; \quad |\mathbf{t}| = 1, \quad (1)$$

where  $\mathbf{t}(s) = \partial \mathbf{r}(s) / \partial s$  is the tangent vector. The energy functional  $H$  is quadratic in the local curvature with  $\kappa$  being the bending stiffness of the chain. The inextensibility of the chain is expressed by the local constraint,  $|\mathbf{t}(s)| = 1$ . This rigid constraint is the source of the difficulty in modeling the statics dynamics of semiflexible polymers. Models that relax the constraint too much – as e.g. the so called Harris-Hearst model (Harris and Hearst, 1966)

– include artificial stretching modes and predict a Gaussian distribution for all spatial distances along the contour; i.e. the essence of semiflexibility has obviously been lost.

Despite the mathematical difficulty of the model some quantities can be calculated exactly. Among these is the tangent-tangent correlation function which decays exponentially,  $\langle \mathbf{t}(s) \cdot \mathbf{t}(s') \rangle = \exp [-(s - s')/\ell_p]$ , with the persistence length  $\ell_p = 2\kappa/((d-1)k_B T)$  in  $d$ -dimensional space. Another example is the mean-square end-to-end distance

$$\langle R^2 \rangle = 2\ell_p^2 (e^{-L/\ell_p} - 1 + L/\ell_p) \quad (2)$$

which reduces to the appropriate limits of a rigid rod,  $\langle R^2 \rangle = L^2$ , and a random coil (with Kuhn length  $2\ell_p$ ),  $\langle R^2 \rangle = 2\ell_p L$ , as the ratio of  $L$  to  $\ell_p$  tends to zero or infinity, respectively. The calculation of higher moments quickly gets very troublesome (Hermans and Ullman, 1952).

In the following we will analyze the wormlike chain model in more detail and determine some of its most important mechanical properties. This is a necessary prerequisite for an understanding of the macroscopic viscoelastic properties of entangled networks.

## II.A Linear force-extension relation

One of the most obvious differences between flexible and semiflexible polymers is their response to external forces. In the flexible case the response is isotropic and proportional to  $1/k_B T$ , i.e., the Hookian force coefficient is proportional to the temperature (a behavior which is known as rubber elasticity). On the other hand when the persistence length is of the same order of magnitude as the contour length, the response becomes increasingly *anisotropic*. Fig. 2 shows the sketch of a semiflexible polymer of fixed length  $L$  with one end clamped at a fixed orientation and a force  $\mathbf{f}$  applied at the other end at an angle  $\theta_0$ . Then the linear response of the chain may be characterized in terms of an effective Hookian spring constant  $k_{\theta_0}$  which depends on the orientation  $\theta_0$  of the force with respect to the tangent vector at the clamped end. Transverse forces give rise to ordinary mechanical bending of the filaments and the *transverse spring coefficient*

$$k_T = \frac{3\kappa}{L^3} \quad (3)$$

is proportional to the bending modulus  $\kappa$ . The linear response for longitudinal forces is due to the presence of thermal undulations, which tilt parts

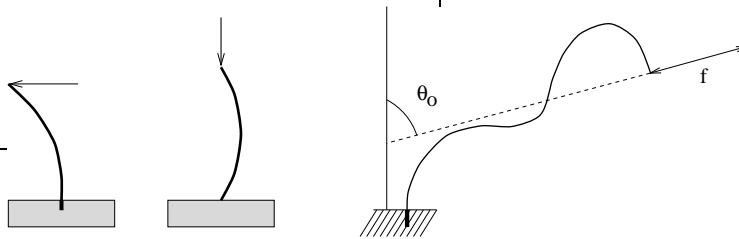


Figure 2: *Left:* The elastic response of a stiff rod is extremely anisotropic due to the Euler instability. *Right:* Response of a filament clamped at one end with a fixed initial orientation to a small external force at the other end.

of the polymer contour with respect to the force direction. The effective longitudinal spring coefficient<sup>1</sup>

$$k_L = \frac{6\kappa^2}{k_B T L^4} \quad (4)$$

turns out to be proportional to  $\kappa^2/T$  indicating the breakdown of linear response at low temperatures ( $T \rightarrow 0$ ) or very stiff filaments ( $\ell_p \rightarrow \infty$ ). This is a consequence of the well known Euler buckling instability illustrated in Fig. 2(left). We note that for the special boundary conditions of a grafted chain (as depicted in Fig. 2) the linear response of the chain can even be worked out exactly for arbitrary stiffness (Kroy and Frey, 1996); these calculations use the fact that the conformational statistics of the wormlike chain is equivalent to the diffusion on the unit sphere (Saitô et al., 1967).

## II.B Nonlinear response

In viscoelastic measurement on *in vitro* actin networks one observes strain hardening (Janmey et al., 1990), i.e. the system stiffens with increasing strain. This may either result from collective nonlinear effects or from the nonlinear response of the individual filaments. In the preceding section we have seen that the force coefficient obtained in linear response analysis for longitudinal deformation diverges in the limit of vanishing thermal fluctuations indicating that the regime of validity for linear response shrinks with

<sup>1</sup>Note that the numerical prefactor in the longitudinal spring coefficient quite sensitively depends on the imposed boundary conditions (here one end clamped at fixed orientation). If we consider a filament with a free hinge the prefactor becomes 90 (MacKintosh et al., 1995) instead of 6.

increasing stiffness. Since the nonlinear response of a single filament may be obtained from the radial distribution function by integration, we discuss the latter first.

A central quantity for characterizing the conformations of polymers is the radial distribution function  $G(\mathbf{R}; L)$  of the end-to-end vector  $\mathbf{R}$ . For a freely jointed phantom chain (flexible polymer) it is known exactly (Yamakawa, 1971) and for many purposes well approximated by a simple Gaussian distribution. While rather flexible polymers can be described by corrections to the Gaussian behavior (Daniels, 1952), the distribution function of polymers which are shorter or comparable to their persistence length shows very different behavior. It is in good approximation given by

$$G(\mathbf{R}; L) \approx \frac{\ell_p}{NL^2} f\left(\frac{\ell_p}{L}(1 - R/L)\right), \quad (5)$$

with

$$f(x) = \begin{cases} \frac{\pi}{2} \exp[-\pi^2 x] & \text{for } x > 0.2 \\ \frac{1/x - 2}{8\pi^{3/2} x^{3/2}} \exp\left[-\frac{1}{4x}\right] & \text{for } x \leq 0.2 \end{cases}$$

and  $N$  a normalization factor close to 1 (Wilhelm and Frey, 1996). This result is valid for  $L \gtrsim 2\ell_p$ ,  $x \gtrsim 0.5$  and  $d = 3$  where  $d$  is the dimension of space. A similar expression exists for  $d = 2$ . As can be seen in Fig. 3, the maximum weight of the distribution shifts towards full stretching as the stiffness of the chain is increased to finally approach a sharp peak at  $R \simeq$  for the rigid rod.

The radial distribution function is a quantity directly accessible to experiment since fluorescence microscopy has made it possible to observe the configurations of thermally fluctuating biopolymers (Gittes et al., 1993; Käs et al., 1993; Ott et al., 1993). Comparing the observed distribution functions with the theoretical prediction is both a test of the validity of the wormlike chain model for actual biopolymers as well as a sensitive method to determine the persistence length which is the only fit parameter. It should be noted here that the determination of persistence length e.g. of actin is still an actively discussed subject (Dupuis et al., 1996; Wiggins et al., 1997).

A very interesting possibility would be to attach two or more markers (e.g., small fluorescent beads) permanently to single strands of polymers and to observe the distribution function of the marker separation. This would eliminate all the experimental difficulties associated with the determination

of the polymer contour. Note that in contrast to existing methods of analysis it is not necessary to know the length of polymer between two markers; it can be extracted from the observed distribution functions along with  $\ell_p$  by introducing  $L$  as a second fit parameter.

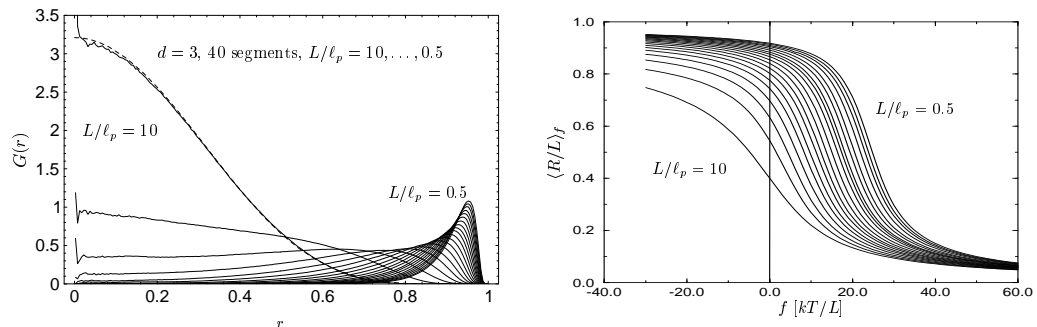


Figure 3: *Left:* End-to-end distribution function of a semiflexible polymer (numerical results). Note that with increasing stiffness of the polymer there is a pronounced crossover from a Gaussian to a completely non-Gaussian from with the weight of the distribution shifting towards full stretching. *Right:* The mean end-to-end distance  $R$  as a function of a force applied between the ends ( $\mathbf{f} = -f\mathbf{R}/|\mathbf{R}|$ ). The step at positive (i.e. compressive) forces can be viewed as a remnant of the Euler instability.

The nonlinear response of the polymer to extending or compressing forces can be obtained from the radial distribution function by integration. The result (Fig. 3) is in agreement with and provides the transition between the previously known limits of linear response and very strong extending forces (e.g., (Marko and Siggia, 1995)). For compressional forces, a pronounced decrease of differential stiffness around the classical critical force  $f_c = \kappa\pi^2/L^2$  can be understood as a remnant of the Euler instability. For filaments slightly shorter than their persistence length the influence of this instability region extends up to and beyond the point of zero force corresponding to the maximum in the linear response coefficient for  $\ell_p \approx L$  (see Fig. 2). For large compressions beyond the instability, the force-extension-relation calculated from the distribution function is only in qualitative agreement with numerical results because of the restricted validity of Eq. 5 for  $x \rightarrow 1$ .

## II.C Single filament dynamics

There are several experimental tools which allow to study the dynamics of single filaments. First of all recent advances in visualizing and manipulating individual macromolecules have provided unique experimental tools (Nagashima and Asakura, 1980; Smith et al., 1992; Ott et al., 1993; Käs et al., 1993; Gittes et al., 1993) for such studies. But also dynamic light scattering experiments (Schmidt et al., 1989; Farge and Maggs, 1993; Götter et al., 1996; Kroy and Frey, 1997a) and micro-rheology with magnetic beads (Zaner and Valberg, 1989; Ziemann et al., 1994; Schmidt et al., 1996; Amblard et al., 1996; Gittes et al., 1997; Mason et al., 1997), which typically are used to study semi-dilute solutions, can to a large extent be understood in terms of single filament dynamics.

Describing the dynamics of semiflexible polymers in solution is complicated by essentially two factors, the chain's local inextensibility (Goldstein and Langer, 1995) and (long-ranged) hydrodynamic interactions mediated by the solvent (Kroy and Frey, 1997a). As we have seen in section II.B the inextensibility of the chain already leads to interesting nonlinear effects for the conformations and the force-extension relation. That this will be even more so in dynamics has been discussed in detail in Ref. (Goldstein and Langer, 1995). In the following we will mainly consider experimental situations where the (external) forces acting on the filament are small and the chains are relatively stiff. This allows us to restrict ourselves to weakly curved conformations, where all nonlinear effects become negligible. If in addition one assumes local viscous forces, i.e. neglects backflow effects, the transverse undulations of the semiflexible chain are governed by the following Langevin equation

$$\zeta_{\perp,0} \frac{\partial}{\partial t} \mathbf{r}_{\perp}(s, t) = -\kappa \frac{\partial^4}{\partial s^4} \mathbf{r}_{\perp}(s, t) + \mathbf{f}_{\perp}(s, t), \quad (6)$$

where  $\zeta_{\perp,0}$  is a local friction coefficient (per length) and the force  $\mathbf{f}_{\perp}(s, t)$  may be either an external force (e.g. exerted by a tweezer) or a random thermal force. In the latter case detailed balance requires

$$\langle f_{\perp}^{\alpha}(s, t) f_{\perp}^{\beta}(s', t') \rangle = 2k_B T \zeta_{\perp,0} \delta^{\alpha\beta} \delta(s - s') \delta(t - t'). \quad (7)$$

In fact, for many purposes the hydrodynamics of the solvent can be comprised into a simple effective friction coefficient  $\zeta_{\perp}$  as a consequence of two scale separations. First, the Brownian dynamics of the polymers are slow

compared to the time scale of the hydrodynamic interactions. So the latter can be assumed to mediate an *instantaneous* interaction. The second simplification is a peculiarity of the rod-like structure of semiflexible polymers. The hydrodynamic interactions only give rise to a very weak (logarithmic) mode number dependence of the local friction. As a consequence, the longitudinal/transverse local friction coefficients can be estimated by (Kroy and Frey, 1997a)

$$\zeta_{\parallel} = \frac{2\pi\eta}{\ln(\xi_h/a)}, \quad \zeta_{\perp} = \frac{4\pi\eta}{\ln(\xi_h/a)},$$

with  $a$  being the diameter of the polymer and  $\xi_h$  defining a second characteristic hydrodynamic length scale. For example, for a free single polymer in solution  $\xi_h$  will depend on the length scale of observation as discussed below in the context of dynamic light scattering. On the other hand, for a polymer in semidilute solution this length dependence saturates at about the mesh size due to screening of the hydrodynamic interactions of this particular polymer through the surrounding network. For the following, we replace the bare friction coefficient  $\zeta_{\perp,0}$  by the renormalized coefficient  $\zeta_{\perp}$ .

The standard procedure of solving the above Langevin equation, Eq. 6, is to look for eigenfunctions (Aragón and Pecora, 1985) which obey boundary conditions appropriate for the particular physical situation under consideration. The corresponding modes of the weakly bending chain are the analog of the Rouse modes for flexible chains (Doi and Edwards, 1986). In the limit of very long chains the characteristic intrinsic time scales of the chain dynamics are set by the decay times  $\tau(q)$  of such Rouse-like modes with wave vector  $q$ ,

$$\tau(q) = \frac{\zeta_{\perp}}{\kappa q^4}, \quad (8)$$

which are immediately read off from Eq. 6 by dimensional analysis. Furthermore, the equipartition theorem tells us that the mean square displacement of a ‘Rouse mode’ is given by

$$\langle r_{\perp}(q, t)r_{\perp}(-q, t) \rangle = \frac{k_B T}{\kappa q^4}. \quad (9)$$

Combining Eqs. 8 and 9 scaling dictates that the correlation function  $\langle r_{\perp}(q, t)r_{\perp}(-q, 0) \rangle$  must be of the form

$$\langle r_{\perp}(q, t)r_{\perp}(-q, 0) \rangle = \frac{k_B T}{\kappa q^4} C(\kappa q^4 t / \zeta_{\perp}). \quad (10)$$

This immediately implies that the mean square displacement of a point  $s$  on the filament shows subdiffusive behavior  $r_{\perp}^2(t) \equiv \langle r_{\perp}(s, t)r_{\perp}(s, 0) \rangle \propto t^{3/4}$ :

$$\begin{aligned} r_{\perp}^2(t) &= \int dq \frac{k_B T}{\kappa q^4} C(\kappa q^4 t / \zeta_{\perp}) \\ &= k_B T \frac{1}{\zeta_{\perp}^{3/4} \kappa^{1/4}} t^{3/4} \int dy y^{-4} C(y^4). \end{aligned} \quad (11)$$

A more quantitative calculation (Kroy and Frey, 1997a) gives

$$r_{\perp}^2(t) = 0.47 (k_B T / \eta \ell_p^{1/3})^{3/4} t^{3/4}, \quad (12)$$

where the numerical prefactor varies slightly with the approximations used to arrive at the above result (Amblard et al., 1996; Granek, 1997). Subdiffusive behavior with such an anomalous power law has recently been observed for the center of mass motion of a bead with diameter  $d$  embedded in an actin solution with a mesh size  $\xi$  larger than the bead diameter (Amblard et al., 1996). It is argued that even if the bead is interacting with several filaments this will only change prefactors but not the exponents of the anomalous diffusion law.

### II.C.1 DYNAMIC LIGHT SCATTERING

A useful experimental technique for investigating the short time dynamics of semiflexible polymers is dynamic light scattering (DLS). In DLS experiments one directly observes the dynamic structure factor

$$g(\mathbf{k}, t) = \frac{1}{N} \sum_{n,m} \langle \exp \{ i\mathbf{k} \cdot (\mathbf{r}_n(t) - \mathbf{r}_m(0)) \} \rangle, \quad (13)$$

where the sum runs over  $N$  equal scattering centers  $n = 1, 2, \dots, N$  (monomers). First, we want to focus on the ideal case of a dilute or semidilute solution of semiflexible polymers, where the scattering wavelength is much smaller than the mesh size. We also assume a separation of length scales,  $a \ll \lambda \leq \ell_p, L$ , i.e., the scattering wavelength  $\lambda$  is large compared to the monomer size  $a$  but small compared to the characteristic mesoscopic scale defined by  $L$  and  $\ell_p$ . As a consequence the contributions to the time decay of  $g(\mathbf{k}, t)$  from center of mass and rotational degrees of freedom of the chain are strongly suppressed as compared to contributions from bending undulations. Moreover, for this case it can be shown (Kroy and Frey, 1997a) that

the structure factor can be written as  $\exp(-k^2 r_{\perp}^2(t)/4)$  with the local mean square displacement  $r_{\perp}^2(t)$  discussed above. From Eq. 11 we immediately obtain the characteristic stretched exponential law

$$g(\mathbf{k}, t) \propto \exp[-(\gamma_k t)^{3/4}] \quad (14)$$

derived by many authors (Frey and Nelson, 1991; Farge and Maggs, 1993; Harnau et al., 1996; Kroy and Frey, 1997a; Granek, 1997). It has been approved experimentally with very high accuracy for F-actin (Götter et al., 1996). However, a more careful analysis reveals that it cannot hold for very short times. For times shorter than  $\zeta/\kappa k^4$  the bending forces can be considered weak and the contour obeys (as far as allowed by the rigid constraint of constant tangent length) the fast wiggling motion imposed by hydrodynamic fluctuations. As a consequence the initial decay of the structure factor is of the form  $g(\mathbf{k}, t) \propto \exp(-\gamma_k^{(0)} t)$  with (Kroy and Frey, 1997a)

$$\gamma_k^{(0)} = \frac{2k_B T}{3\pi\zeta_{\perp}} k^3 = \frac{k_B T}{6\pi^2\eta} k^3 \ln(e^{5/6}/ka). \quad (15)$$

(The last equation (Kroy and Frey, 1997a), provides an explicit expression for the above mentioned logarithmic effects of the hydrodynamic interaction.) For polymers, which are not quite as stiff as actin, e.g. for so called intermediate filaments, this initial decay regime is readily observed in light scattering experiments. Analyzing the data by Eq. 15 allows one to estimate the friction coefficient  $\zeta_{\perp}$  entering the Langevin equation Eq. 6 or, equivalently, the thickness  $a$  of these filaments. (P. Janmey has recently obtained quite accurate values for the diameter of vimentin by this method (Janmey, 1997).)

The friction coefficient is an important input parameter, if the stretched exponential law of Eq. 14 shall be used for a quantitative analysis of the filament stiffness. To this end, the prefactor  $\gamma_k$  in Eq. 14 must be determined. Various slightly differing values for  $\gamma_k$  are available in the theoretical literature (Farge and Maggs, 1993; Götter et al., 1996; Harnau et al., 1996; Kroy and Frey, 1997a; Granek, 1997) reflecting different approximations in the calculation. As we mentioned above, the accuracy of the value obtained for the persistence length by this method is also limited by the accuracy of ones knowledge of the input parameters, in particular by the friction coefficient  $\zeta_{\perp}$ . If both the initial decay and the stretched exponential regime can be detected, it is possible to use the friction coefficient determined via Eq. 15

together with  $\gamma_k = (\Gamma(1/4)/3\pi)^{4/3} k_B T k^{8/3} / \zeta_{\perp} \ell_p^{1/3}$  in Eq. 14. The accuracy of this method in determining the persistence length has not yet been explored in practice. It can be used in any case to study relative differences in  $\ell_p$  (Götter et al., 1996).

If the condition  $\lambda \ll \xi_m$  assumed above does not hold, the form of the dynamic structure factor is affected by steric constraints and hydrodynamic screening effects. The latter lead to a saturation of the  $k$ -dependence of the friction coefficient  $\zeta_{\perp}$  given in Eq. 15, presumably at about  $k \simeq \xi_m^{-1}$ . The steric constraints can give rise to more dramatic effects. One observes a slowing down of the long time decay of the structure factor and even a saturation at a finite value (named ‘Debye-Waller factor’ by solid state physicists). This reflects the cage effect caused by the surrounding network (see discussion below). Strictly speaking, the notion of a ‘Debye-Waller factor’ is only justified in a crosslinked gel, where the spatial correlations can not decay further. For a solution one should rather speak of an elastic plateau. Scattering techniques could be a valuable tool in exploring this plateau complementary to the mechanical rheological methods mentioned below, and a quantitative theory is currently being worked out. A simple method to account for the cage effect is to redo the above analysis with an additional term  $\gamma r_{\perp}$  (representing a tube-like harmonic confinement force) in the Langevin equation Eq. 6. This is, however, not sufficient to explain the experimental data. A more realistic model includes a term for the collective dynamics of the background medium and eventually also filament tension accounting for crosslinks and entanglements (the cage is not really a homogeneous tube). The theoretical analysis as well as the pertinent experiments are still in a preliminary stage.

DLS experiments are a useful experimental method to answer some biologically relevant questions. Recently it was found (Goldmann et al., 1997) that the decay of the dynamic structure factor is slowed down with increasing talin concentration. This can be attributed to a talin induced cross-linking of actin filaments and formation of actin bundles. Similar results are obtained with a talin tail fragment, but not with a head fragment. Especially for strong talin concentrations a reduction in relaxation rate of about an order of magnitude is observed and the shape of the curves deviates strongly from the stretched exponential of Eq. 14. This is in sharp contrast to proteins that cause a stiffening of F-actin, such as the tropomyosin/troponin complex (Götter et al., 1996). In the latter case the relaxation rate is shifted but the functional form is not affected, as expected from the dependence of  $\gamma_k$

on persistence length. On the other hand, for low talin concentrations the curves for  $g(k, t)$  are quite similar to those with tropomyosin/troponin. It is tempting to attribute this observation to the formation of single bundles, which could behave similar to stiffened F-actin. However, such speculations are dangerous if not supported by independent structural analysis. Dynamic light scattering is a sensitive quantitative method when escorted by an appropriate model. But it is also a highly ambiguous probe, not well suited for the exploration of unknown structures.

### II.C.2 COLLOIDAL PROBES AND MICRO-RHEOLOGY

As we have seen in the preceding section dynamic light scattering allows us to probe the single chain dynamics and attain information on the mean-square displacement. It is however an indirect method in the sense that the dynamic structure factor involves a summation over all monomers in the sample. A complementary method would be to study the local dynamics by direct imaging methods. One quite successful approach has been to attach fluorescent labels to the actin filament and watch its motion using video microscopy (Käs et al., 1994); this enabled a direct measurement of the self-diffusivity by reptation. Instead of labeling a whole filament one has also started using micron-sized particles embedded in the network to learn about the viscoelastic properties (Ziemann et al., 1994; Amblard et al., 1996; Gittes et al., 1997; Schnurr et al., 1997). These micro-rheological methods are local probes but through collisions still couple to a large number of filaments in the network. In order to learn about the single filament dynamics one would like to use colloidal particles much smaller than the mesh-size which are attached to a single filament and exert point forces. Such an idealized micro-rheological experiment has recently been performed on a semiflexible polymer networks consisting of microtubules (Caspi et al., 1998). An analogous study for F-actin networks is currently being analyzed (Dichtl and Sackmann, 1998).

In the experiments of the microtubule networks (Caspi et al., 1998) the subdiffusive behavior of the segment dynamics is clearly observed at sufficiently small times. Using Eq. 12 even allows for a quantitative measurement of the persistence length of microtubules ( $\ell_p \approx 7\mu\text{m}$ ). For larger times the mean-square displacement showed saturation indicating some effective tube potential due to the topological constraints imposed by the surrounding filaments. Preparing a stressed network and hence changing the filament dynamics from bending to tension dominated the mean-square segment displace-

ment also showed the expected behavior with  $\langle(\mathbf{r}_\perp(s, t) - \mathbf{r}_\perp(s, 0))^2\rangle \propto \sqrt{t}$ . With further advances in experimental resolution these type of experiments have a great potential in yielding important information on the dynamics of F-actin networks in time-domains which have up to date not been accessible.

### III VISCOELASTICTY OF BIOPOLYMER NETWORKS

One the basis of our understanding of the static and dynamic properties of single actin filaments we are now in a position to analyze the by far more complicated problem of the microscopic basis for the macroscopic viscoelastic properties of solutions and gels of semiflexible polymers. For networks consisting of flexible polymers we have a rather good understanding of the polymer dynamics on the molecular level based on ideas like entanglements, the tube model and reptation theory (de Gennes, 1971; Doi and Edwards, 1978). In this section we will discuss how some of these quite successful concepts can be applied or have to be modified for semiflexible polymer networks.

#### III.A Experimental techniques and results

Remarkable progress has been achieved in our qualitative and quantitative understanding of the viscoelasticity of semiflexible polymer solutions. This is mainly due to the advances and new developments in experimental techniques. In the following we describe some of the main experimental tools and the results obtained by it. Part of the discussion of the experimental results is deferred to section III.B where it will be analyzed in terms of the theoretical models presented.

##### III.A.1 MACRO-RHEOLOGY

One of the best known method to study the viscoelastic properties of polymeric liquids is *macroscopic rheometry* using a *rotating disc rheometer*. There have been a large number of experimental investigations on F-actin solutions based on this classical rheological techniques (Sato et al., 1985; Zaner and Hartwig, 1988; Janmey et al., 1988; Müller et al., 1991; Janmey, 1991; Pollard et al., 1992; Wachsstock et al., 1993; Newman et al., 1993; Ruddies et al., 1993; Janmey et al., 1994). There are various types of measurements one can make with those rheometers. In the creep mode the creep compliance can be measured in a time window of  $t = 10^{-1} - 10^4$  s, which gives more reliable values of the long time behavior of the network viscoelasticity. In the

oscillatory mode the dynamic storage and loss moduli,  $G'(\omega)$  and  $G''(\omega)$ , can be measured in the frequency range  $\omega/2\pi = 10^{-5} - 10$  Hz. Fig. 4 shows the typical frequency dependence of the storage  $G'(\omega)$  and loss modulus  $G''(\omega)$  of an F-actin solution with gelsolin at monomer concentration  $c = 0.4$  mg/ml measured by a rotation disc rheometer (Hinner and Sackmann, 1998). The

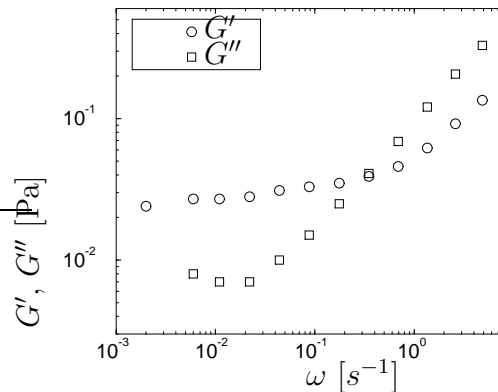


Figure 4: Frequency dependence of the storage  $G'(\omega)$  and loss modulus  $G''(\omega)$  of an F-actin solution with gelsolin at monomer concentration  $c = 0.4$  mg/ml.

measurement was performed over four frequency decades; they show that the response of the network depends on how fast one pulls. In *physical networks* where there are no permanent crosslinks between the filaments one can roughly discern three different regimes as a function of the frequency of the external perturbation. In an intermediate frequency range, usually slightly below 1 Hz, the solution shows elastic behavior and obeys Hook’s law with a linear relation  $\sigma = G\gamma$  between stress  $\sigma$  and strain  $\gamma$ . At frequencies above this “rubber plateau” the storage and loss modulus both show a power-law dependence on the frequency. Below the rubber plateau (at large time scales) the solution shows viscous behavior and obeys Newton’s law  $\sigma = \eta\dot{\gamma}$ , where the stress is proportional to the strain rate  $\dot{\gamma}$ . The latter regime is absent in *chemical networks* where crosslinking proteins like  $\alpha$ -actinin and talin prevent large scale relative motion of the actin filaments (Wachsstock et al., 1994). In Fig. 4 we merely see the onset of the terminal relaxation regime at the lower end of the experimentally accessible frequency window. The latter regime is, however, readily observed by creep measurements.

Unfortunately however, these macro-rheological studies did not lead to a coherent picture of the viscoelastic properties. To the contrary the reported

rheological parameters, in particular the magnitude of the plateau value, are pretty disperse. A discussion of these discrepancies which may be partly due to difficulties in purification and sample preparation has been given (Janmey et al., 1994).

More recent experiments (Tempel et al., 1996; Hinner et al., 1998) and micro-rheological measurements discussed below show consistently low values for the plateau modulus in the range of several tenth of a Pa depending on concentration and length distribution of the filaments. Why other experiments find elastic moduli higher by a factor of 1000 is not clear at present. For a discussion of these recent data we refer the reader to section III.B.

### III.A.2 MICRO-RHEOLOGY

Over the last few years new *micro-rheological techniques* have been developed which allow the tracking or manipulation of sub-micrometer particles. Actually these type of methods have quite a long history. The first documented usage of magnetic particles to investigate the local viscoelastic properties of biomaterials dates back to 1922 when magnetic particles were manipulated by field gradients in the cytoplasm of the cell (Heilbronn, 1922) and in gelatin (Freundlich and Seifriz, 1922). Subsequently magnetic beads have been used to study the creep response of the cytoplasm (Crick and Hughes, 1950; Sato et al., 1984) and the viscosity of *Amoeba* protoplasm (Yagi, 1961). More recently magnetic bead techniques have been applied to study the viscoelasticity of F-actin networks (Zaner and Valberg, 1989) and the vitreous body of the eye (Lee et al., 1993).

By now there are two different types of microrheological setups, which either measure the correlation or response function of micron sized beads embedded in the network. Of course, due to the fluctuation-dissipation theorem both techniques should yield equivalent results though differences might exist related to the spatial and temporal resolutions which can be achieved. The magnetic bead rheometer (Ziemann et al., 1994; Schmidt et al., 1996) and magnetic tweezer methods (Amblard et al., 1996) manipulates micron sized magnetic beads by magnetic field gradients. Other methods employ *passive* observation of the thermal fluctuations (Brownian motion) of the probe particles (Gittes et al., 1997; Schnurr et al., 1997; Mason et al., 1997). These methods also differ by the detection method of the particle displacements. In all magnetic-bead techniques one uses video microscopy, while the Michigan group (Gittes et al., 1997; Schnurr et al., 1997) employs laser inter-

ferometry with a resolution less than 1 nm. Yet another method to observe thermal fluctuations of ensembles of particles is *diffusive wave spectroscopy* (DWS) (Mason and Weitz, 1995). But, in contrast to the methods described above DWS measures average and not local viscoelastic properties.

A central question in using these type of techniques is whether and how the local response of the probe is related to the macroscopic modulus. One line of thinking is to assume that the bead is embedded in a continuum viscoelastic medium (Ziemann et al., 1994). Taking into account the finite radius  $R$  of the bead (Schnurr et al., 1997) one finds (for an incompressible medium) that there is simple relation between the macroscopic shear modulus  $G^*(\omega)$  and the response function of the bead  $\alpha(\omega)$  given by  $\alpha(\omega) = 1/6\pi G^*(\omega)R$ . The applicability of such a continuum approach may, however, be questioned. A different line of argument is based on a more molecular picture where the beads push against individual filaments which themselves collide with other filaments (Amblard et al., 1996). This relates the observed modulus to single filament dynamics and in particular to the subdiffusive segment dynamics discussed in section II.C. But, as already noted above the actual relation between the observed linear response function of the beads and the viscoelastic properties of the medium awaits a theoretical description on a more molecular level which includes both network and solvent dynamics. It may well be that micro-rheology and macro-rheology are complementary experimental probes sensitive to different modes and aspects of the complex viscoelastic behavior of semiflexible polymer networks.

### III.B Theoretical modeling

In order to describe the material properties of the cytoskeleton, one has to understand how semiflexible polymers built up statistical networks and how stresses and strains are transmitted through such networks. In particular one would like to understand how the network responds to time-dependent macroscopic (macro-rheology) or local (micro-rheology) deformations probed by the experimental methods described in the preceding section. Note that it is a priori not evident whether micro- and macro-rheology are probing the same kind of network deformations or are sensitive to different aspects of the network elasticity. Since the cytoskeleton contains a broad variety of crosslinking proteins one would also like to understand how the mechanical and dynamical properties of these proteins influence the viscoelasticity of the network (Wachsstock et al., 1994; Tempel et al., 1996). Fig. 5 shows a sketch

of a solution of semiflexible polymers with (right) and without (left) chemical crosslinks, respectively.

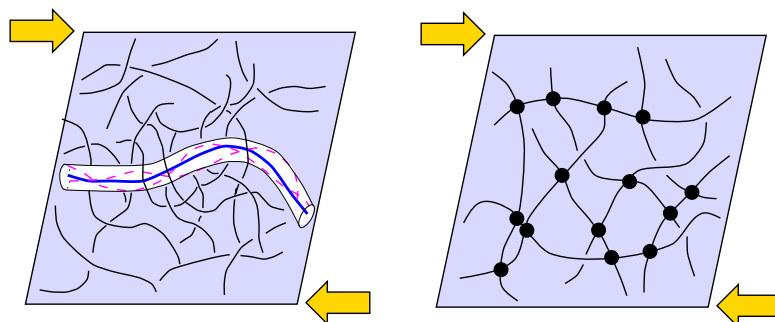


Figure 5: Sketch of a physical (*left*) and a chemical (*right*) network. In physical networks the rotational and translational motion of an individual test-polymer is severely hindered by steric interactions with neighboring polymers. Anticipating a time scale separation between internal bending modes and the center of mass motion of the filaments these topological restrictions lead to a *cage* or *tube* of a cylindrical structure. In chemical networks permanent connections between the filaments due to some cytoskeletal proteins like  $\alpha$ -actinin or talin lead to additional constraints on the degrees of freedom of an individual chain. Arrows indicate an externally imposed macroscopic deformation of the network.

In conventional polymer systems made up of long flexible chain molecules the viscoelastic response is *entropic* in origin over a wide range of frequencies (Doi and Edwards, 1986). For semiflexible polymers a complete understanding of the viscoelastic response is complicated by several factors. First of all, there are several ways by which forces can be transmitted in a network. This can either happen by steric (or solvent-mediated) interactions between the filaments (i.e. “collisions”) or by viscous couplings between the filaments and the solution. It is a priori not at all obvious which if any of these coupling will dominate. In the case of flexible polymers it is generally believed that macroscopic stresses are transmitted in such a way that these transformations stay affine locally, i.e. that the end-to-end distance of a single filament follows the macroscopic shear deformation (Doi and Edwards, 1986). Implicit in this hypothesis is the assumption that there is a very strong viscous coupling between polymers and solution and that inter-polymer forces can be neglected. As a consequence most of the viscoelastic properties are modeled by a single-filament picture. The applicability of such a single-filament

theory to semiflexible polymer networks may be seriously questioned. Second, as we have seen in section II, single filaments are *anisotropic elastic elements* showing quite different response for forces perpendicular or parallel to its mean contour. Therefore one has to ask what kind of deformation of the actin filament is the dominant one and whether due to the anisotropy of the building blocks of the network macroscopically affine deformations stay affine locally.

### III.B.1 TYPICAL LENGTH AND TIME SCALES; THE TUBE PICTURE

A good starting point for a theoretical analysis of the viscoelastic properties of semiflexible polymer solutions is to consider the typical time and length scales.

The *persistence length*  $\ell_p$  and the *total contour length*  $L$  are the two intrinsic length scales of a single filament. A gross characterization of the network architecture is the *geometrical mesh-size*  $\xi_m$ ; it may be defined as  $\xi_m = \sqrt{3/\nu L}$  where  $\nu$  is the number of polymers per unit volume. Typical networks show a *separation of length scales* such that  $\ell_p \gg \xi_m$ . Hence each polymer is surrounded by a large number of other polymers leading to a severe restriction of its ability to move transverse to its mean contour. This cage effect also restricts the undulations of the filament on length scales larger than a certain length  $L_e$ , called the *deflection length* or *entanglement length*, which characterizes the typical distance between two collision points of a “test-polymer” with the surrounding chains. If one approximates the effect of the surrounding medium by a cylindrical tube of diameter  $d$  (of the order of magnitude of the mesh size) the entanglement length is given by Odijk’s estimate (Odijk, 1983)

$$L_e^3 \simeq d^2 \ell_p. \quad (16)$$

Actually, previous fluorescence microscopic observations (Käs et al., 1994) seem to have virtually confirmed the existence of such a cylindrical tube or cage. Physical networks of *flexible* polymers have very successfully been described by *reptation theory* (Doi and Edwards, 1986) which uses the tube concept quite extensively. In this approach one picks a test-polymer and models the influence of all the surrounding polymers by an effective potential, called the *reptation tube*. The test-polymer is of course itself part of the reptation tubes for various other polymers in its neighborhood. Thus reptation theory is a mean-field or molecular field like approach as it can be

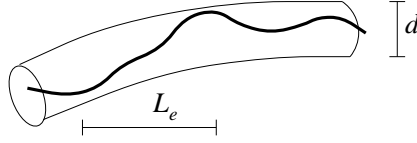


Figure 6: Intuitive view of the cage effect in semidilute solutions of semiflexible polymers. A test polymer is confined to a tube with diameter  $d$ . For a wormlike chain  $L_e^3 \simeq d^2 \ell_p$  (Odijk, 1983).

found in many other areas of physics. In the following we will adapt the tube picture to semiflexible polymer networks and see how far this will carry us in understanding its viscoelastic properties.

There are also a number of interesting time scales in semiflexible polymer solutions. In sections II.C we already discussed the shortest of these time scales, namely the relaxation times  $\tau(q) = \zeta_{\perp}/\kappa q^4$  for thermal undulations with wave vector  $q$ . These time scales are accessible by dynamic light scattering and microrheology and for wave length in the range of  $0.1\mu\text{m}$  to  $1\mu\text{m}$  they are of the order of magnitude  $1\mu\text{sec}$  to  $1\text{msec}$ . Next we have a time scale  $\tau_e$  which a single filament needs to equilibrate within the tube. This can be estimated as the time a segment on the filament needs to wander a mean square distance of the order of the tube diameter  $d$

$$d^2 = r_{\perp}^2(t) \propto \frac{t^{3/4}}{\kappa^{1/4} \zeta^{3/4}}. \quad (17)$$

Theoretical estimates give that  $\tau_e$  is of the order of 50 ms for a tube-diameter of  $0.2\mu\text{m}$ . For larger times there should be an interesting crossover from single filament dynamics to collective networks dynamics which is at present largely unexplored. Future research should certainly concentrate on this time window in order to shed some light on the physical principles which lead to the elastic plateau. The longest time scale  $\tau_r$  of the problem is determined by the diffusion constant for the center of mass motion of the semiflexible polymer in the disordered actin mesh (reptation time). This is also the time scale at which the actin solution shows viscous behavior which is of the order of hours (Hinner et al., 1998). Obviously there is a huge gap between the equilibration time  $\tau_e$  of a filament within a tube and the reptation time  $\tau_r$ . There might be several other time scales which fill this gap and mark transitions from a dynamics dominated by transverse

undulations to a dynamics dominated by longitudinal stress relaxation within the tube (Isambert and Maggs, 1996). But up to now all arguments about the existence and nature of these intermediate time scales are nothing but very speculative ideas.

In the following we will concentrate on a description of present theoretical models in the three major regimes, which is (1) the “rubber plateau”, (2) the terminal regime and (3) the high-frequency region.

### III.B.2 THE “RUBBER PLATEAU”

If solutions of semiflexible polymers are sufficiently dense and are probed at sufficiently short time scales (typically in the range of  $10^{-2}$  Hz to 1 Hz) they will exhibit a so-called “*rubber plateau*” where the storage modulus  $G'(\omega)$  becomes nearly frequency independent. Already the existence of such a plateau and hence an elastic response of a network in the absence of permanent crosslinks is a nontrivial observation. In general it is traced back to the fact that in sufficiently dense polymer solutions the center of mass motion of a single filament is severely constrained by its neighboring filaments such that there is a *time scale separation* between the internal dynamics and the center of mass motion of the polymers. The topological constraints due to the uncrossability of the polymers are termed *entanglements* and are despite their transient nature thought to act in much the same way as permanent crosslinks over the time scales in the plateau region.

Even by anticipating a separation of time scales and neglecting the center of mass motion the calculation of the plateau modulus is still a complicated statistical mechanics problem. One has to answer the question how in a disordered network macroscopic stresses and strains are transmitted to individual filaments. This requires an understanding of the coupling of the shear flow in the solvent to the filament dynamics as well as the solvent-mediated or direct steric interaction between the filaments. However little is known about these matters. Present theoretical approaches all use a single-chain picture where very different assumptions are made on the effect of the topological constraints on the conformation of a single filament.

In what might be called the *affine model* the so called “phantom model” of rubber-elasticity (Treloar, 1975) is adopted to semiflexible polymer systems (MacKintosh et al., 1995). It is assumed that upon deforming the network macroscopically the path of a semiflexible polymer between two entanglement points is straightened out or shortened in an affine way with the sample. The

macroscopic modulus is then calculated from the free energy cost associated with the resulting change in the end-to-end distance. Since in a solution forces between neighboring polymers can only be transmitted transverse to the polymer axis and there is no restoring force for sliding of one filament past another, it is however hard to imagine that entanglements are able to support longitudinal stresses in filaments.

The modulus predicted in the affine model should scale as  $G^0 \propto c^{11/5}$  and leads to absolute values of the order of 10 Pa; such high values are at odds with the low values observed in recent experiments on F-actin solutions (Hinner et al., 1998). It was therefore argued (MacKintosh and Janmey, 1997) that such models are more appropriate for crosslinked networks, where they would predict a plateau value  $G^0 \simeq k_B T \ell_p^2 / \xi_m^5$ . But, even in such chemical networks with crosslinks present it is a priori not obvious that local deformations on the scale of a single filament are actually affine and that longitudinal stresses in the filaments are the dominant contribution to the plateau modulus. Because of the strongly anisotropic behavior of the single elements, a detailed investigation of the stress propagation in crosslinked networks is necessary to determine the dominant deformation mode<sup>2</sup>.

The second approach to explain the observed plateau modulus employs the *tube picture* in which each strand is confined within a cylindrical tube. Recent theoretical and experimental studies (Isambert and Maggs, 1996; Hinner et al., 1998) based on pioneering work from the 80's (Helfrich and Harbich, 1985; Odijk, 1986; Semenov, 1986) suggest a different view. The basic idea can be formulated in a way reminiscent of a well known effect in granular media. A randomly packed granular material increases its volume upon shearing (see Fig. 7). In the polymer solution, the analogue of the granules are the *tubes* of Fig. 6, which are a theoretical representation of the average volume avail-

---

<sup>2</sup>In section III.B.5 we will consider *disordered* networks to address a key aspect of the geometrical structure of both cellular and artificial stiff polymer networks. Specifically, we use a crosslinked network of sticks randomly placed in a plane as a toy model for studying the origin of macroscopic elasticity in a stiff polymer network. Although quantitative predictions about the behavior of existing (three-dimensional) networks of semiflexible polymers are not attempted at this stage, this model is expected to reflect the salient features of the full problem and to promote its understanding by allowing the detailed discussion of questions like “What modes of deformation contribute most to the network elasticity?”, “How many filaments do actually carry stress, how many remain mostly unstressed?”, “What kind of effective description of the complicated microscopic network geometry should be used?”. This approach connects the theory of cytoskeletal elasticity to the very active fields of transport in random media and elastic percolation.

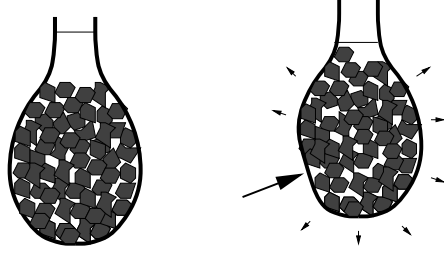


Figure 7: Reynolds experiment. Upon shearing an elastic bottle filled with granular material and water the random packing of the granules is distorted. As a consequence there are additional voids which in turn lead to a *decrease* in the water level.

able to the unconstrained contour undulations of wavelength shorter than a characteristic length  $L_e$ , known as *deflection length* or *entanglement length*, respectively. As the granules, the tubes are not space filling despite having an optimum random packing in equilibrium. A shear deformation disturbs this optimum packing, leading to an expansion of the granular medium but to tube compression in the polymer solution, because in the latter the total volume (not the tube volume) is conserved. This intuitive argument suggests to express the shear modulus in close analogy to the osmotic pressure in terms of a virial expansion in the polymer concentration  $c_p$ ,

$$G^0 = k_B T c_p (1 + B_2 c_p \dots) . \quad (18)$$

To determine the second virial coefficient  $B_2$  we follow Onsager (Onsager, 1949) and estimate the number of mutual collisions of the tubes  $B_2 c_p = L/L_c$  (which we have rewritten by introducing the collision length  $L_c$ ) by the excluded volume  $d(L - L_c)^2$  divided by the available volume  $\xi_m^2 L$  per polymer. In the excluded volume we have subtracted  $L_c$  to account for the reduced efficiency of dangling ends to contribute to the plateau modulus.  $L_c$  is determined by the consistency requirement that the number of mutual collisions of the tubes be equal to the number of collisions of the enclosed polymer with its tube. After all, the tube is a mere theoretical concept representing the physical interactions between polymers. Using Eq. 16 to substitute the tube diameter  $d$  we obtain the curved line shown in Fig. 8. With  $\ell_p = 17 \mu\text{m}$  the optimum fit was obtained with  $\xi_m = 0.25 \mu\text{m}$  and a prefactor of 1.4 to  $B_2$  in Eq. 18. This can be considered nice agreement at the present level of experimental accuracy.

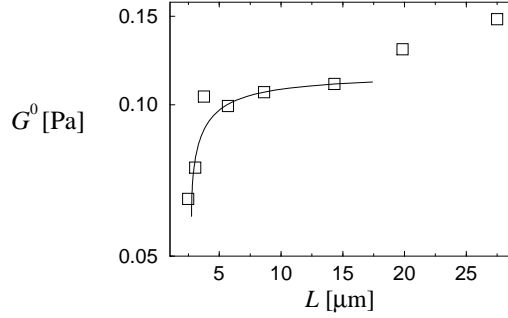


Figure 8: The plateau modulus above the entanglement transition as a function of polymer length for constant monomeric actin concentration  $c = 1.0$  mg/ml. The increase of  $G^0$  for large  $L$  is not yet fully understood. Taken from (Hinner et al., 1998).

We now turn to a different argument for estimating the plateau modulus which we think is better suited for a more quantitative analysis. Here one considers the free energy cost of suppressed transverse fluctuations of the polymers that comes about by an affine deformation of the tube diameter. As noted above the mean distance between collisions of a tagged polymer with its surrounding tube with diameter  $d$  is given by  $L_e \simeq \ell_p^{1/3} d^{2/3}$ , see Eq. 16. Since each of these collisions reduces the conformation space it cost free energy of the order of  $k_B T$  the total free energy of  $\nu = c/L$  polymers per unit volume becomes

$$F \simeq \nu k_B T \frac{L}{L_e}. \quad (19)$$

To be able to compare these results to experiments one needs to know how the tube diameter  $d$  depends on the concentration of the solution or equivalently on the mesh size  $\xi_m := \sqrt{3/\nu L}$ . In other words we have to determine the average thickness  $d$  of a bend cylindrical tube in a random array of polymers as depicted in Fig. 9. The contour and thickness of the tube will be determined by a competition between bending energy favoring a thin straight tube and entropy favoring a curved thick tube. This competing effects define a characteristic length scale which is nothing but the Odijk deflection length  $L_e$  defined above. For length scales below  $L_e$  the tube will be almost straight and we can estimate its thickness as follows. Upon restricting the orientations of the polymers to being parallel to the coordinate axes the density

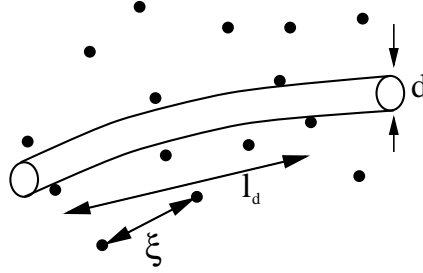


Figure 9: Sketch of a cylindrical tube in a random array of polymers (indicated by black dots) with average distance  $\xi_m$ .

of intersection points (black dots in Fig. 9) will be  $1/\xi^2$ . Hence for a tube of length  $L_e$  the line density of these intersection points projected to a line perpendicular to the tube increases as  $L_e/\xi_m^2$  which implies that the tube diameter decreases with increasing tube length as

$$d \simeq \xi_m^2/L_e. \quad (20)$$

Combining Eq. 20 and 16 one finds  $L_e = (\xi_m^2 \ell_p^{1/2})^{2/5}$  leading to the following form of the free energy and hence the plateau modulus  $G^0$  as a function of temperature, concentration and the intrinsic stiffness of the filament parameterized by the persistence length

$$G^0 \simeq F \simeq k_B T \ell_p^{-1/5} c^{7/5}. \quad (21)$$

The above scaling law is included as a limiting case in a more detailed analysis concerned with the calculation of the absolute value of the plateau modulus (Wilhelm and Frey, 1998a).

Recent experiments seem to favor the above tube picture, where the plateau modulus is thought to arise from free energy costs associated with deformed tubes due to macroscopic stresses. Fig. 10 shows the results of a recent measurement of the concentration dependence of the plateau modulus in F-actin solutions (Hinner et al., 1998) which confirms the scaling prediction  $G^0 \propto c^{7/5}$  quite unambiguously. A much stronger dependence on concentration – as predicted by a purely mechanical model (Satcher and Dewey, 1996) or by the affine model discussed above (MacKintosh et al., 1995) – is not in accordance with the data in Fig. 10.

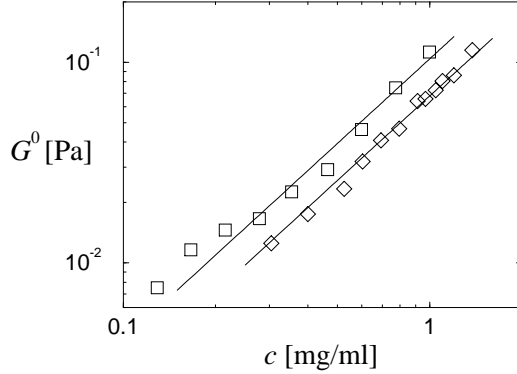


Figure 10: Concentration dependence of the plateau modulus of pure actin (open squares) and actin with a small amount of gelsolin ( $r_{AG} = 6000 : 1$ ) corresponding to an average actin filament length  $L = 16 \mu\text{m}$  (open diamonds). The straight lines indicate the power  $7/5$ . Taken from (Hinner et al., 1998).

### III.B.3 TERMINAL RELAXATION

At frequencies below the plateau regime the elastic response decreases and the polymer solution starts to flow. The corresponding time scale is called the terminal relaxation time. It can be determined from the measured plateau modulus and the zero shear rate viscosity using the relation  $\eta_0 = \pi^2 G^0 \tau_r / 12$  or from the frequency dependent moduli. The zero shear rate viscosity is a well defined property of the solution but it is difficult to measure if  $\tau_r$  is very large. The frequency, where  $G' = G^0/2$  is sometimes used as an easier accessible substitute. For actin both definitions of  $\tau_r$  have been shown to lead to the same results (Tempel, 1996). However, the experimental results do not agree with previous theoretical predictions (Odijk, 1983; Doi, 1985).

Intuitively, the mechanism for the terminal relaxation seems obvious from the tube picture (see Fig. 6) described above: viscous relaxation only occurs, when the polymers have time to leave their tube-like cages by Brownian motion along their axis. If the polymers perform a one dimensional diffusion along a fixed path, the overlap with the original tube decays only slowly (as  $1/\sqrt{t}$ ), because the polymer enters its old tube frequently. Only changes in orientation lead to exponential stress relaxation. If we assume that the stresses in the solution are proportional to the fraction of the polymers in their original tubes, we conclude that the terminal relaxation time is equal to the time calculated by Odijk and Doi (Odijk, 1983; Doi, 1985). In the stiff

limit we thus expect

$$\tau_r = \frac{L\ell_p}{4D_{\parallel}}. \quad (22)$$

Here  $D_{\parallel}$  denotes the longitudinal diffusion coefficient derived from the friction coefficient  $\zeta_{\parallel}L$  introduced above via Einstein's relation  $D_{\parallel} = k_B T / \zeta_{\parallel}L$ . As we already mentioned before, this prediction is not supported by recent experiments on actin solutions (Tempel, 1996). Rather these data seem to suggest the relation

$$\tau_r \simeq \frac{L(L + 2\ell_p)^2}{D_{\parallel}} \quad (23)$$

with a persistence length  $\ell_p \approx 17 \mu\text{m}$ . In this expression the tube length is

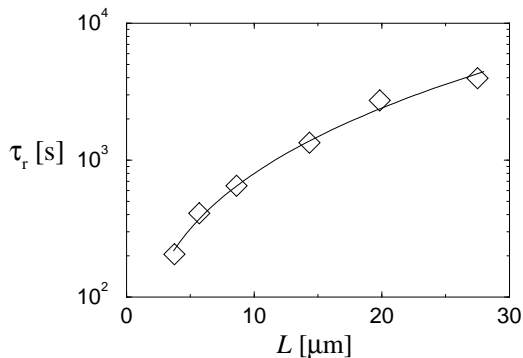


Figure 11: Terminal relaxation time above the entanglement transition (Hinner et al., 1998). The curved line is a fit by Eq. 23.

augmented by the persistence length at each end. This result is not easily interpreted theoretically. It can be obtained (Kroy and Frey, 1997b) from the assumption that the stress does decay when the polymer has lost its original orientation while moving along a fixed path (i.e., it is not allowed to penetrate the tube walls). The slow algebraic stress decay implied by this interpretation seems to be supported qualitatively by the slow decay of the viscoelastic moduli at low frequencies. However, without further experimental and theoretical investigations, Eq. 23 can at present only be regarded as a phenomenological parameterization.

#### III.B.4 HIGH FREQUENCY BEHAVIOR

At frequencies above the “rubber plateau” (i.e. above 1 Hz for a typical F-actin solution) an anomalous power-law increase of the storage and loss

modulus with frequency,  $G'(\omega) \propto G''(\omega) \propto \omega^{3/4}$ , has been observed in various recent experiments (Amblard et al., 1996; Gittes et al., 1997; Schnurr et al., 1997).

This power-law dependence of the shear modulus seems to be a generic feature of any semiflexible polymer solution at high frequencies. It is tempting to speculate that this universal power-law is somehow tightly connected with the anomalous subdiffusive behavior of the segment dynamics of a single filament. But in view of the actual micro-rheological experiments, where one observes the mean-square displacement of a bead of diameter larger than the mesh-size and hence couples to a large number of filaments, it is not obvious how this comes about. A thorough understanding would need to explore the nature of the crossover from local dynamics dominated by filament undulations to the collective dynamics of the network and the solvent.

At present there are two different theoretical approaches based on different assumptions on the nature of the dominant excitations of the individual filaments generated by the beads embedded in the network.

In one class of theoretical models one simply takes over the “phantom model” approach for the plateau modulus to the high frequency behavior (Gittes and MacKintosh, 1998; Morse, 1998). It is assumed that under an applied shear deformation the filaments undergo affine deformations on a length scale of order  $L_e$  implying longitudinal stresses on single filaments. This leads to a simple relation between the macroscopic shear modulus  $G(\omega)$  and the longitudinal single filament response  $\alpha(\omega)$ ,

$$G(\omega) = \frac{1}{15} \nu L_e / \alpha(\omega) - i\omega\eta. \quad (24)$$

The longitudinal response function is found to be

$$\alpha(\omega) = \frac{1}{k_B T q_1^4 \ell_p^2} \sum_{n=1}^{\infty} \frac{1}{n^4 - i\omega/2\omega_1}, \quad (25)$$

where  $q_1 = \pi/L_e$  and  $\omega_1 = (\kappa/\zeta)(\pi/L_e)^4$  are the relaxation rate and wave-vector of the slowest mode, respectively. By construction of the model this reduces to the plateau modulus  $G^0 \simeq 6\nu k_B T \ell_p^2 / L_e^3$  (MacKintosh et al., 1995) at low frequencies, whose validity for entangled solution is questionable (see the discussion in section III.B.2). In the high frequency regime  $\omega \gg \omega_1$  one gets (Gittes and MacKintosh, 1998; Morse, 1998)

$$G^*(\omega) = \frac{1}{15} \nu (k_B T)^{1/4} \ell_p^{5/4} (i\omega\zeta_{\perp})^{3/4}. \quad (26)$$

Note that this high frequency behavior of the plateau modulus is independent of the entanglement length  $L_e$ , but solely depends on the persistence length of a single filament and the lateral friction coefficient  $\zeta_{\perp}$ . The theoretical analysis reproduces the experimentally observed power-law dependence. However, due to the generic nature of this power law, which is a direct consequence of mode-spectrum of semiflexible polymers, this agreement may be completely fortuitous. A real check of the theoretical model can be achieved by comparing the theoretically estimated and experimentally measured amplitudes of this power-law. A recent estimate (Gittes and MacKintosh, 1998) suggests that the amplitude of the affine model is off by a factor of about seven.

A complementary theoretical approach starts from the picture of an idealized micro-rheological experiment, where a point force  $\mathbf{f}_s = \mathbf{f}\delta(s)$  is applied to the polymers by optical or magnetic tweezers techniques. This would require beads much smaller than the mesh-size which are tightly connected with the filaments. Such a setup is hard to achieve but some recent experimental studies point in this direction (Dichtl and Sackmann, 1998). The equation of motion for the transverse undulations are then given by Eq. 6. Such an ansatz has been used before (Amblard et al., 1996) to explain the experimentally observed subdiffusive segment diffusion in entangled F-actin solutions. Note that this scaling behavior can already be inferred from the observation that the dynamic structure factor of single semiflexible polymers decays as  $\exp[-(\gamma t)^{3/4}]$  for scattering wavelengths much smaller than the persistence length. This was measured in light scattering experiments (Götter et al., 1996) and explained theoretically (Frey and Nelson, 1991; Farge and Maggs, 1993; Kroy and Frey, 1997a) in terms of Eq. 6. From the fluctuation dissipation theorem and the Kramers-Kronig-relations one concludes  $G' = (\sqrt{2} - 1)G'' \propto \omega^{3/4}$ . The prefactor of this high-frequency modulus which is now mainly due to transverse instead of longitudinal modes differs from Eq. 26 by a factor of order  $\xi_m/\ell_p$ , i.e. it is much smaller. This would be contrary to the above model, where longitudinal deformations dominate, lead to a modulus (per polymer) which not only depends on the intrinsic properties of the individual filaments but through the mesh-size also depends on the density of the polymer solution. Which one of these theoretical models is superior to the other is hard to tell. It may well be that the actual physical mechanism is different from both. There is certainly a tremendous need for more detailed experimental studies which not only measure the power-law dependence of the modulus but also determine the concentration dependence

of the prefactor.

### III.B.5 EFFECT OF CROSSLINKING

In a crosslinked network it is obviously possible in principle that longitudinal deformations (changes in the end-to-end distance) are enforced upon single filaments under strain. For very regular networks such as a triangular lattice the force constant  $k_L$  associated with such deformations will dominate the macroscopic moduli since no strain of the network without a change of the end-to-end distances is possible and<sup>3</sup>  $k_L/k_T = 60\ell_p/L_c \gg 1$  at the relevant lengthscale  $L_c \ll \ell_p$  where  $L_c$  is the typical distance between crosslinks.<sup>4</sup> It is, however, possible to imagine network structures where the opposite extreme is realized and the softer bending modes dominate completely — see, e.g., (Satcher and Dewey, 1996). Naturally, this will lead to a very different prediction for the elastic modulus of the network. It is not easy to see which case is realized in less ideal structures with a significant amount of disorder such as in typical cytoskeleton networks.

To study this problem we consider the following two dimensional toy model: sticks of length  $L$  are placed randomly with regard to position and orientation on a square piece of the plane. Wherever two sticks intersect they are connected by a crosslink with zero extensibility. The crosslinks can either be chosen to fix the relative orientation of the rods as well (“stiff crosslinks”) or not (“flexible crosslinks”). The elasticity of the rods is determined by their Young’s modulus  $E$  and radius  $r = a/2$  leading to  $k_{L0} = \pi r^2 E/L_c$  and  $k_{T0} = (3/4)\pi r^4 E/L_c^3 = k_T$ . While this is a  $T = 0$  model it captures the essential feature  $k_L/k_T = (4/3)L_c^2/r^2 \gg 1$  for sensible densities of the network. Note that the lengthscale  $L_c$  below which  $k_L > k_{L0}$  is  $L_c \approx (45r^2\ell_p)^{1/3} \approx 0.3 \mu\text{m}$  for actin such that the force constants used in this model can even be assumed to be realistic for relatively dense networks as they are found in the cytoskeleton.

Periodic boundary conditions are applied and a shear deformation is enforced by shifting the boundary conditions between the upper and lower edges of the square. The elastic response of the network is calculated using the method of finite elements. By construction, the undeformed network is

---

<sup>3</sup>Note that the exact prefactors depend on and will change with the boundary conditions chosen.

<sup>4</sup>A second crossover will take place at very short lengthscales  $L_c \approx a$  with  $a$  the filament diameter, where the bending modulus will become comparable to the elastic longitudinal compressibility of actin.

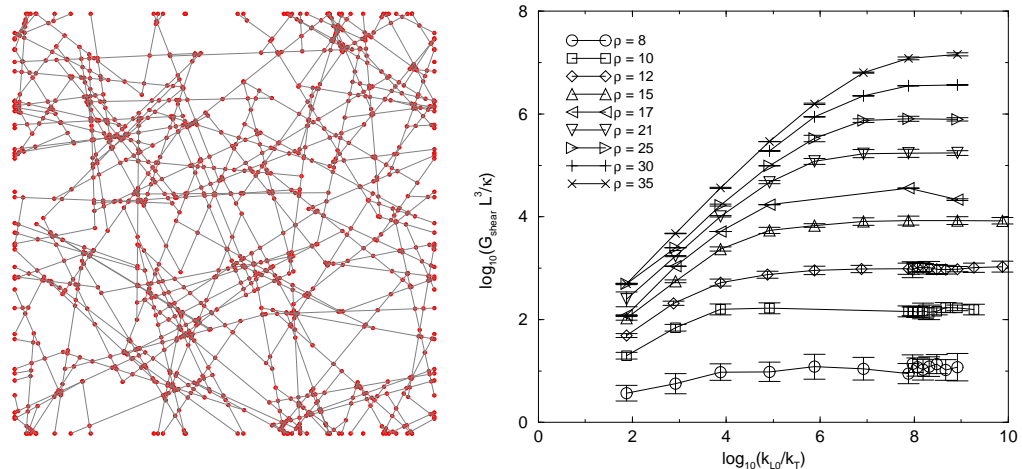


Figure 12: *Left:* Geometry of a sticks network for density  $\rho = 30$  and system size  $L_s = 2$ . *Right:* Dependence of the shear modulus on the ratio  $k_{L0}/k_T$  of compressional to bending stiffness for constant  $k_T$  for networks with  $L_s = 15$  and flexible crosslinks. Use of fixed crosslinks does not affect the result for densities sufficiently above the percolation threshold. The error bars given indicate the standard deviation of the modulus for different realizations of the network. Zero errorbars correspond to only one sample.

not prestressed. In the following discussion we chose the rod length  $L$  as unit length and  $\kappa/L^3$  as unit for the elastic modulus. The independent parameters of the system are the density  $\rho$  of rods per area  $L^2$ , the system size  $L_s$  and the aspect ratio  $\alpha = r/L$  of the rods. If we are not too close to the geometric percolation threshold  $\rho_c \approx 5.71$  (Pike and Seager, 1974) the modulus  $G$  is independent of system size  $L_s$  for moderately large systems. For the results presented below we chose  $L_s = 15$ .

To address the question whether the elasticity of a random stiff polymer network is dominated by transverse or by longitudinal deformations of the filaments, we study the dependence of the shear modulus on the ratio of the two force constants. Keeping  $k_T$  fixed we increase  $k_{L0}$  from values corresponding to  $\alpha \approx 0.1$  (thick rod) to values corresponding to  $\alpha \approx 10^{-5}$  (slender rod) for different system densities (see Fig. 12). We observe that beyond a certain point the shear modulus ceases to depend on  $k_{L0}$ , indicating that the elasticity is dominated by bending modes for slender rods (see Fig. 12). Since

the characteristic lengths in the network decrease with increasing density, the point of onset for this behavior shifts upwards with density. The dominance of bending modes in this region is confirmed by the observation that almost all of the energy stored in the deformed network is accounted for by the transverse deformation of the rods.

While these two-dimensional results are certainly not straightforwardly applicable to three-dimensional networks we will nevertheless try to get a feeling for the scales involved. Network densities can be compared roughly by using the average distance  $L_c$  between intersections as a measure: A cytoskeletal network might have  $L_c \approx 0.1 \mu\text{m}$  with typical filament lengths of  $2 \mu\text{m}$  corresponding to a two-dimensional density of  $\rho \approx 20$  and an aspect ratio of  $\alpha \approx 0.002$  resp.  $k_{LO}/k_T \approx 10^{-5}$ . Comparison with Fig. 12 shows that this would just place the network in the bending dominated regime. This might, however, be different for different scales or if more order is present in the network than assumed here. The key point we want to make is that the mechanics of a crosslinked network of stiff elements is already quite a complicated problem without an obvious effective model. For a more detailed analysis of the random stick model we refer the interested reader to Ref. (Wilhelm and Frey, 1998b).

#### IV CONCLUSIONS AND OPEN PROBLEMS

We have seen that the cytoskeleton is a composite biomaterial with a wide variety of interesting viscoelastic properties. In particular F-actin solutions and networks provide a model system for a polymeric liquid composed of semiflexible polymers which is accessible to a complementary set of experimental techniques ranging from direct imaging techniques over dynamic light scattering to classical rheological methods. From these studies it has become quite obvious that semiflexible polymer networks require new theoretical models different from conventional theories for rubber elasticity. The nature of the entanglement in solutions of filaments is very different from flexible coils. In a frequency window where an elastic plateau is observed the topological (steric) hindrance between the filaments does not support any longitudinal stresses along the filaments. A model based on the tube picture and the free energy costs associated with deformations of the tube diameter leading to a restricted conformation space for the transverse undulations seems to be sufficient to explain the observed concentration dependence of the plateau modulus. Recent more detailed theoretical models even allow

for a quantitative comparison with the absolute value of this modulus. Outside the rubber plateau in the high-frequency as well as the low-frequency regime the situation is less clear. In the latter regime the classical description by Doi leads to a dependence of the terminal relaxation time which is at odds with the experimental data. Micro-rheology and dynamic light scattering experiments allow us to access the short-time dynamics of the filaments within a network. Here a theoretical model which describes the combined dynamics of network and solvent in this regime is still lacking. At present there are two quite different approaches which either start from a continuum medium approximation or from a single-filament picture. Obviously both are just limiting cases and a molecular theory needs to explain how starting from the single-filament dynamics including interactions with the solvent and the neighboring filaments leads at some length and time scale to collective behavior, which might be described in terms of some continuum model.

Another very important question is concerned with the effect of chemical crosslinks on the mechanical properties of semiflexible polymer networks. This is of prime interest for both cell biology and for polymer science. In cell biology one would like to know how the material properties (e.g. elastic modulus, time scales for structural rearrangement and stress propagation) change as a function of the network architecture and the mechanical and dynamic properties of the crosslinks. From the perspective of polymer science it connects cytoskeletal elasticity with the very active fields of transport in random media and elastic percolation. In section III.B.5 we have presented a numerical study using a two-dimensional toy model of sticks randomly placed on a plane and crosslinked at their mutual intersection points. One can certainly not expect that such a simplified model leads to quantitative results, but we think that some of its main features carry over to the more complicated situation of a three-dimensional network. Future research may concentrate on extending these studies to three-dimensional networks and study how distribution of crosslinks and different network architectures affect the elastic modulus.

## ACKNOWLEDGMENTS

This work has been supported by the Deutsche Forschungsgemeinschaft through a Heisenberg Fellowship (No. Fr 850/3) and through the group grants (Sonderforschungsbereiche) SFB 266 and SFB 413. Some of the experimental re-

sults described here were obtained in collaboration with Erich Sackmann and his coworkers. We are very grateful for these collaborations, as well as for the stimulating discussions with Paul Janmey and Rudolf Merkel.

## REFERENCES

- Amblard, F., A. C. Maggs, B. Yurke, A. N. Pargellis, and S. Leibler. 1996. *Phys. Rev. Lett.*, 77:4470.
- Aragón, S. R. and R. Pecora. 1985. *Macromol.*, 18:1868.
- Caspi, A., M. Elbaum, R. Granek, A. Lachish, and D. Zbaida. 1998. *Phys. Rev. Lett.*, 80:1106–1109.
- Crick, F. H. C. and A. F. W. Hughes. 1950. *Exp. Cell Res.*, 1:37–80.
- Daniels, H. E. 1952. *Proc. Roy. Soc. Edinburgh*, 63A:290.
- de Gennes, P. G. 1971. *J. Chem. Phys.*, 55.
- des Cloizeaux, J. and G. Jannink. 1990. *Polymers in Solution*. Clarendon Press, Oxford.
- Dewey, C. F., S. Bussolari, M. Gimbrone, and P. F. Davies. 1981. *J. Biochem. Eng.*, 103:177–185.
- Dichtl, M. and E. Sackmann. 1998. Local and long range reptation motion of semiflexible macromolecules in entangled networks studied by colloidal probes. Unpublished.
- Doi, M. 1985. *J. Pol. Sci. Pol. Symp.*, 73:93–103.
- Doi, M. and S. F. Edwards. 1978. *J. Chem. Soc. Faraday Trans. II*, 74:1789.
- Doi, M. and S. F. Edwards. 1986. *The Theory of Polymer Dynamics*. Clarendon Press, Oxford.
- Dupuis, D. E., W. H. Guiford, and D. M. Warshaw. 1996. *Biophys. J.*, 70:A268.
- Farge, E. and A. C. Maggs. 1993. *Macromol.*, 26:5041.
- Ferry, J. D. 1980. *Viscoelastic Properties of Polymers*. John Wiley & Sons, New York.
- Freundlich, H. and W. Seifriz. 1922. *Z. Phys. Chem.*, 104:223.
- Frey, E. and D. R. Nelson. 1991. *J. Phys. I France*, 1:1715–1757.
- Gittes, F. and F. C. MacKintosh. 1998. Dynamic shear modulus of semiflexible polymer networks. Unpublished.
- Gittes, F., B. Mickey, J. Nettleton, and J. Howard. 1993. *Journal of Cell Biology*, 120:923.
- Gittes, F., B. Schnurr, P. D. Olmsted, F. C. MacKintosh, and C. F. Schmidt. 1997. *Phys. Rev. Lett.*, 79:3286.
- Goldmann, W. H., Z. Guttentberg, S. Kaufmann, D. Hess, R. M. Ezzell, and G. Isenberg. 1997. *Eur. J. Biochem.*, 250:447–450.
- Goldstein, R. E. and S. A. Langer. 1995. *Phys. Rev. Lett.*, 75:1094.

- Götter, R., K. Kroy, E. Frey, M. Bärmann, and E. Sackmann. 1996. *Macromol.*, 29:30.
- Granek, R. 1997. *J. Phys. II France*, 7:1761–1788.
- Harnau, L., R. G. Winkler, and P. Reineker. 1996. *J. Chem. Phys.*, 140:6355.
- Harris, R. A. and J. E. Hearst. 1966. *J. Chem. Phys.*, 44:2595.
- Heilbronn, A. 1922. *Jahrb. Wiss. Bot.*, 61:284–338.
- Helfrich, W. and W. Harbich. 1985. *Chem. Scr.*, 25:32.
- Hermans, J. J. and R. Ullman. 1952. *Physica*, 44:2595.
- Hesketh, J. E. and I. F. Pryme, editors. 1995. *The Cytoskeleton: Structure and Assembly*, volume I. Jai Press.
- Hinner, B. and E. Sackmann. 1998. unpublished.
- Hinner, B., M. Tempel, E. Sackmann, K. Kroy, and E. Frey. 1998. Entanglement, elasticity and viscous relaxation of actin solutions. unpublished.
- Isambert, H. and A. C. Maggs. 1996. *Macromol.*, 29:1036.
- Janmey, P. A. 1991. *J. Biochem. Biophys. Methods*, 22:41–53.
- Janmey, P. A. 1997. private communication.
- Janmey, P. A., S. Hvidt, F. George, J. Lamb, and T. Stossel. 1990. *Nature*, 347:95.
- Janmey, P. A., S. Hvidt, J. Käs, D. Lerche, A. Maggs, E. Sackmann, M. Schliwa, and T. P. Stossel. 1994. *J. Biol. Chem.*, 269:32503.
- Janmey, P. A., S. O. Hvidt, J. Peetermans, J. Lamb, J. D. Ferry, and T. P. Stossel. 1988. *Biochemistry*, 27:8218–8227.
- Käs, J., H. Strey, M. Bärmann, and E. Sackmann. 1993. *Europhysics Letters*, 21:865.
- Käs, J., H. Strey, and E. Sackmann. 1994. *Nature*, 368:226.
- Käs, J., H. Strey, J. Tang, D. Finger, R. Ezzell, E. Sackmann, and P. Janmey. 1996. *Biophys. J.*, 70:609.
- Kishino, A. and T. Yanagida. 1992. *Nature*, 334:74.
- Kratky, O. and G. Porod. 1949. *Rec. Trav. Chim.*, 68:1106.
- Kroy, K. and E. Frey. 1996. *Phys. Rev. Lett.*, 77:306.
- Kroy, K. and E. Frey. 1997a. *Phys. Rev. E*, 55:3092.
- Kroy, K. and E. Frey. 1997b. Viscoelasticity of gels and solutions of semiflexible polymers. unpublished.
- Lee, B., M. Litt, and G. Buchsbaum. 1993. *Biorheology*, 29:521–534.
- MacKintosh, F. and P. A. Janmey. 1997. *Curr. Op. Cell. Biol.*, 2:350–357.
- MacKintosh, F., J. Käs, and P. Janmey. 1995. *Phys. Rev. Lett.*, 75:4425.
- Marko, J. F. and E. D. Siggia. 1995. *Macromol.*, 28:8759.
- Mason, T. G., K. Ganesan, J. H. van Zanten, D. Wirtz, and S. C. Kuo. 1997. *Phys. Rev. Lett.*, 79:3282.
- Mason, T. G. and D. A. Weitz. 1995. *Phys. Rev. Lett.*, 74:1250.
- Morse, D. 1998. Viscoelasticity of tightly entangled solutions of semi-flexible poly-

- mers. unpublished.
- Müller, O., H. E. Gaub, M. Bärmann, and E. Sackmann. 1991. *Macromol.*, 24:3111.
- Nagashima, H. and S. Asakura. 1980. *J. Mol. Biol.*, 136:169.
- Newman, J., K. S. Zaner, K. L. Schick, L. C. Gershman, L. A. Selden, H. J. Kinoshian, J. L. Travis, and J. E. Estes. 1993. *Biophys. J.*, 64:1559–1566.
- Odijk, T. 1983. *Macromol.*, 16:1340.
- Odijk, T. 1986. *Macromol.*, 19:2313.
- Onsager, L. 1949. *Ann. N. Y. Acad. Sci.*, 51:627.
- Ott, A., M. Magnasco, A. Simon, and A. Libchaber. 1993. *Phys. Rev. E*, 48:R1642.
- Pike, G. E. and C. H. Seager. 1974. *Phys. Rev. B*, 10:1421.
- Pollard, T. D., I. Goldberg, and W. H. Schwarz. 1992. *J. Biol. Chem.*, 267:20339–20345.
- Ruddies, R., W. H. Goldmann, G. Isenberg, and E. Sackmann. 1993. *Eur. Biophys. J.*, 22:309–321.
- Saitô, N., K. Takahashi, and Y. Yunoki. 1967. *J. Phys. Soc. Jap.*, 22:219.
- Satcher, Jr., R. L. and C. F. Dewey, Jr. 1996. *Biophys. J.*, 71:109–118.
- Sato, M., G. Leimbach, W. Schwarz, and T. Pollard. 1985. *J. Biol. Chem.*, 260:8585–8592.
- Sato, M., T. Wong, D. T. Brown, and R. D. Allen. 1984. *Cell Motil.*, 4:7–23.
- Schliwa, M. 1985. *The Cytoskeleton: An Introductory Survey*. Springer Verlag, Berlin.
- Schmidt, C., M. Bärmann, G. Isenberg, and E. Sackmann. 1989. *Macromol.*, 22:3638.
- Schmidt, F. G., F. Ziemann, and E. Sackmann. 1996. *Eur. Biophys. J.*, 24:348–353.
- Schnurr, B., F. Gittes, F. C. MacKintosh, and C. F. Schmidt. 1997. *Macromol.*, 30:7781–7792.
- Semenov, A. N. 1986. *J. Chem. Soc. Faraday Trans.*, 86:317.
- Smith, S. B., L. Finzi, and C. Bustamante. 1992. *Science*, 258:1122.
- Tempel, M. 1996. *Aktinbindende Proteine als Membran/Zytoskelett-Koppler und als Modulatoren der Viskoelastizität von Aktinnetzwerken*. PhD thesis, Technische Universität München.
- Tempel, M., G. Isenberg, and E. Sackmann. 1996. *Phys. Rev. E*, 54:1802.
- Treloar, L. R. G. 1975. *The Physics of Rubber Elasticity*. Clarendon Press, Oxford.
- Wachsstock, D., W. Schwarz, and T. Pollard. 1993. *Biophys. J.*, 65:205–214.
- Wachsstock, D., W. Schwarz, and T. Pollard. 1994. *Biophys. J.*, 66:801.
- Wiggins, C. H., D. X. Rivelino, A. Ott, and R. E. Goldstein. 1997. Trapping and wiggling: Elastohydrodynamics of driven microfilaments. cond-mat/9703244.
- Wilhelm, J. and E. Frey. 1996. *Phys. Rev. Lett.*, 77:2581.
- Wilhelm, J. and E. Frey. 1998a. Absolute value of the plateau modulus of semiflexible polymer solutions. in preparation.

- Wilhelm, J. and E. Frey. 1998b. Elasticity of stiff polymer networks. in preparation.
- Yagi, K. 1961. *Comp. Biochem. Physiol.*, 3:37–91.
- Yamakawa, H. 1971. *Modern Theory of Polymer Solutions*. Harper & Row, New York.
- Zaner, K. S. and J. H. Hartwig. 1988. *J. Biol. Chem.*, 263:4532–4536.
- Zaner, K. S. and P. A. Valberg. 1989. *J. Cell Biol.*, 109:2233–2243.
- Ziemann, F., J. Rädler, and E. Sackmann. 1994. *Biophys. J.*, 66:2210.